

Performance of the Automated Adjoint Accelerated MCNP (A³MCNP) for Simulation of a BWR Core Shroud Problem

A. Haghghat, H. Hiruta and B. Petrovic

Penn State University

Nuclear Engineering Program

University Park, PA 16802

haghgha@gracie.psu.edu; hiruta@gracie.psu.edu; petrovic@gracie.psu.edu

J. C. Wagner

Holtec International

555 Lincoln Drive West

Marlton, NJ 08053

johncwagner@compuserve.com

Abstract

This paper discusses the recently developed version of MCNP, A³MCNP, that automatically prepares variance reduction parameters based on the CADIS (Consistent Adjoint Driven Importance Sampling) methodology. A³MCNP prepares necessary information for performing 3-D deterministic adjoint transport calculations. This automation includes (1) generation of a 3-D mesh distribution, (2) preparation of input files for cross-section generation and the adjoint transport calculation, calculation of a biased source, and (3) calculation of weights for the weight-window space and energy splitting/roulette. A³MCNP has been used to analyze deep-penetration shielding applications. Here, we discuss its use for determining neutron-induced displacement per atom (DPA) at BWR core shroud welds. We have obtained DPA values with 1% (1- σ) uncertainties in less than 5 CPU hours, whereas an analog Monte Carlo simulation we estimate would require about one month of CPU time. Furthermore, performance of the code has been measured for different discrete deterministic adjoint models.

1. Introduction

For deep penetration particle transport simulations, the statistical Monte Carlo and deterministic Sn methods are widely used.[1] Each method has specific advantages, and one can be more effective than the other for certain applications and objectives. Monte Carlo is considered to be a more accurate methodology, because it does not require any approximation in geometric representation and energy treatment of nuclear interactions. However, it requires a significant amount of computation time for achieving statistically reliable results. The S_N method is generally faster and generates detailed information; however, because of computer memory limitations, approximations to the geometry and energy treatment are necessary.

For real-life 3-D deep penetration problems, the analog Monte Carlo is not practical, and the variance reduction ("biasing") techniques are needed. Techniques such as weight-window splitting/roulette, exponential transformation, and source biasing can be very effective, if a "good" set of parameters is available. These parameters have to be selected by the user, and generally are difficult to estimate, especially for a large complex simulation.

It has long been recognized that the particle "importance" is related to the particle statistical weight, and therefore can be used to estimate the variance reduction parameters. Further, it is known that the adjoint linear Boltzmann equation can be solved for estimation of the particle "importance". Various groups and organizations have developed different methodologies for estimation of the particle "importance" and its utilization for variance reduction. Conveyou et al. [2] developed an inverse relation between particle statistical weight and its "importance", and showed the merits of the importance function for transport and source biasing. Kalos [3] described the importance-sampling technique and its relation to a weight function and a zero-variance solution. Tang et al. [4] applied the 1-D deterministic S_N adjoint solution for a shipping cask simulation with the MORSE code.[5] Miller et al. [6] developed an automatic importance generator for geometric splitting based on a diffusion calculation and have incorporated it into the MCBEND code.[7] Mickael [8] developed a version of the MCNP code [9] that performs an adjoint diffusion calculation to generate weight-window parameters for nuclear-well-logging calculations. Turner and Larsen [10] described the local importance function transform method, which uses a deterministic adjoint to bias distance-to-collision and selection of post-collision energy group and direction for multigroup Monte Carlo calculations. Van Ripper et al. have developed the AVATAR method [11] that uses the inverse of "importance" function from a three-dimensional adjoint calculation to determine space-, energy-, and angular-dependent weight windows. We have developed the CADIS (Consistent Adjoint Driven Importance Sampling) methodology [12,13] that uses a 3-D S_N adjoint function for source biasing and consistent transport biasing with the weight-window technique. We have used the concept of importance sampling to derive a consistent relation between source-biasing parameters and weight-window lower bounds (for transport biasing). We have incorporated the CADIS methodology into the MCNP code and achieved excellent performance. Further, we have automated calculation of the deterministic adjoint function by developing a new version of MCNP, A^3 MCNP (Automated Adjoint Accelerated MCNP) [13,14] that automatically:

- i) Generates a mesh distribution for a 3-D deterministic adjoint calculation;
- ii) Prepares material and composition files for multigroup cross section generation;
- iii) Prepares an input file for the deterministic TORT code [15];
- iv) Prepares a biased source and space-energy dependent weight-window lower bounds based on the CADIS methodology.

A^3 MCNP has been used to analyze deep-penetration shielding applications.[12,13,16] In this paper, we utilize the A^3 MCNP code to determine the DPA (displacement per atom) at a BWR core shroud weld. This work is being performed as part of a larger project aimed at investigating the role of irradiation on the observed cracks in the core shroud welds. The problem requires performing neutron and gamma transport throughout a large, complex three-dimensional model. We will measure the performance of A^3 MCNP for different three-dimensional discrete adjoint models.

Section 2 discusses the theory of CADIS methodology. Section 3 describes the utilization of A^3 MCNP. Section 4 describes the core shroud problem. Section 5 discusses the performance of A^3 MCNP for different discretized deterministic models. Section 6 summarizes and concludes the paper.

2. Theory - CADIS Methodology

In this Section, we briefly review the theory of CADIS (Consistent Adjoint Driven Importance Sampling) methodology, which develops formulations for source and transport biasing using a space-energy dependent weight-window technique. These formulations are presented below.

2.1 Source biasing

In most Monte Carlo simulations, one is interested in estimating a response (e.g., flux, dose, reaction rate) in a phase-space ($dEd\Omega dV$). This is equivalent to solving the following integral:

$$R = \int_p \psi(p) \sigma_d(p) dp, \quad (1)$$

where ψ is the particle flux and σ_d is an objective function in phase-space about $(r, E, \Omega) \in p$. Following commutation between the "forward" and "adjoint" transport equations, for a vacuum boundary condition, an alternative formulation for the response R reads as

$$R = \int_p \psi^+(p) q(p) dp, \quad (2)$$

where ψ^+ and q are the adjoint ("importance") function and source density, respectively.

To solve this integral with the Monte Carlo method, particles are sampled from $q(p)$ which may not necessarily be the best pdf for the objective of interest. From the "importance sampling" method [17], we may show [13] that the biased pdf that minimizes the variance in R is given by

$$\hat{q}(p) = \frac{\psi^+(p) q(p)}{\int_p \psi^+(p) q(p) dp}, \quad (3)$$

and the corresponding particle statistical weight that results in conserving the expected number of particles is given by

$$W(p) = \frac{R}{\psi^+(p)}. \quad (4)$$

2.2 Transport biasing

To obtain a formulation for transport biasing, we start with the integral form of the linear Boltzmann equation given by

$$\psi(p) = \int K(p' \rightarrow p) \psi(p') dp' + q(p), \quad (5)$$

where $[K(p' \rightarrow p) dp'] dp'$ is the expected number of particles emerging in dp about p from events in dp' about p' , and $q(p)$ is the source density. Following some algebraic manipulations, we may rewrite above equation as

$$\hat{\psi}(p) = \int \hat{K}(p' \rightarrow p) \hat{\psi}(p') dp' + \hat{q}(p), \quad (6)$$

where

$$\hat{\psi}(p) = \frac{\psi^+(p) \psi(p)}{\int \psi^+(p) q(p) dp}, \quad (7)$$

and

$$\hat{K}(p' \rightarrow p) = K(p' \rightarrow p) \left[\frac{\psi^+(p)}{\psi^+(p')} \right]. \quad (8)$$

Since $K(p' \rightarrow p)$ is not known, we simulate the particle transport between events in the normal way and alter the number of particles emerging in p from an event in p' by the ratio of the importances ($\psi^+(p)/\psi^+(p')$). This means that if the ratio is > 1 , particles are created (splitting), while if the ratio is < 1 , particles are killed (roulette). To preserve the expected number of particles, the particle statistical weight following the transport is modified according to

$$W(p) = W(p') \left[\frac{\psi^+(p')}{\psi^+(p)} \right] \quad (9)$$

In the CADIS methodology, we utilize Eqs. 3 and 4 for calculating source biasing parameters, and Eqs. 8 and 9 for calculating transport biasing parameters (for the weight-window technique). Note that the word "consistent" in CADIS refers to our consistent use of the "importance sampling" method in deriving the above equations.

3. Implementation of CADIS in MCNP

The CADIS methodology is utilized to calculate source and transport biasing parameters for the weight-window technique. To implement the CADIS methodology, MCNP was modified to perform the following major tasks:

- i) Reading the "importance" function and preparing a biased source based on Eq. (3)
- ii) Superimposing the deterministic S_n spatial-mesh distribution and energy-group structure onto the Monte Carlo model in a "transparent" manner;
- iii) Calculating space- and energy-dependent weight-window lower bounds (W_l) for the "transparent" space-energy mesh according to

$$W_l(r, E) = \frac{R}{\phi^+(r, E)} \cdot \frac{1}{\left(\frac{C_u + 1}{2} \right)}$$

where ϕ_+ is the scalar adjoint function, $C_u = W_u/W_l$ is the ratio of upper and lower weight window values.

- iv) Updating the particle weight, as each particle is transported through the "transparent" mesh.

4. Development of A³MCNP, and its use

To utilize the CADIS methodology, one has to develop a mesh distribution and a multi-group cross section file for performing a 3-D discrete ordinates (S_N) adjoint deterministic calculation. This, however, is not straightforward and requires a significant amount of time and knowledge. To remove this difficulty, a revised version of the MCNP code, A³MCNP (Automated Adjoint Accelerated MCNP) has been developed. A³MCNP performs the following tasks:

- i) Generation of a mesh distribution for the deterministic S_n calculation. (Mesh generator utility first generates a uniform mesh distribution to extract information on material distribution, and then through a back-thinning process prepares a variable mesh distribution.)
- ii) Preparation of input file for the TORT S_n code.
- iii) Determination of material compositions and preparation of the necessary input files for the GIP code [18] for generation of multi-group cross sections.

The flowchart below presents the steps performed in an A³MCNP simulation.

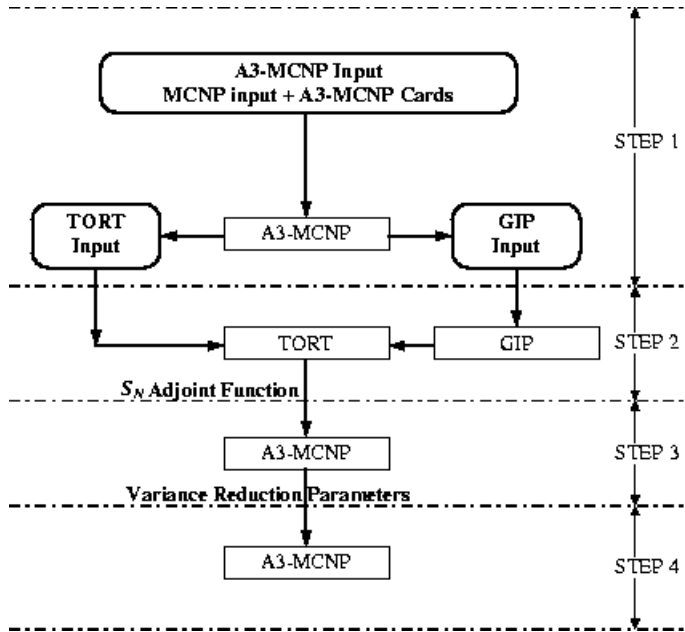


Fig. 1 - Flowchart for the use of A³MCNP code

5. Description of the BWR Core Shroud Problem

The core shroud is a ~5 cm thick stainless steel annulus located between the core and the pressure vessel of a BWR reactor. Fig. 2a shows the axial locations of the core-shroud welds (H1 to H9) relative to the reactor core and other structural components. Fig. 2b shows the radial position of the core shroud relative to the core and the jet pumps.

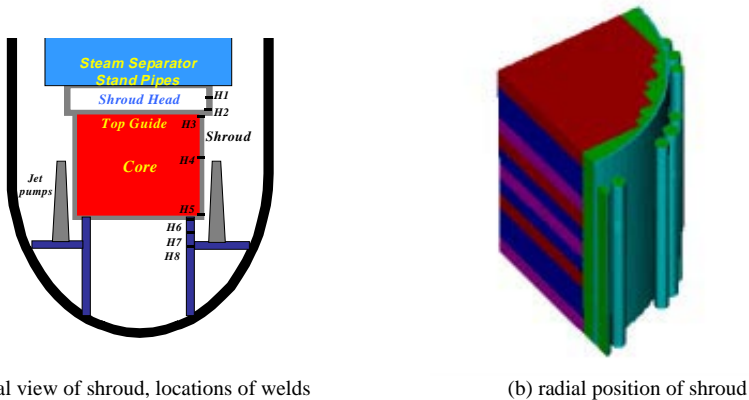


Fig. 2 - Schematic of a BWR Core Shroud

The goal of this project is to determine neutron and gamma flux distributions and the amount of displacement per atom (DPA) at H2, H3, and H4 welds. Since welds are located above and below the core, and gamma rays are generated within the structural materials through (n, γ) interactions (mainly from thermal neutrons), it is necessary to simulate neutrons of all energies (0 to 20 MeV) and gamma rays in a 3-D model. In this paper, we will only discuss our simulations for the H4 weld that is located at ~63.5 above the core mid-plane (see Fig. 2a). We have developed a model of size 300x300x381 cm³.

Here, we determine the DPA at a small segment (2x2x2 cm³) of the H4 weld. (Note that we consider that the weld width (axially) is 2 cm.) To prepare multi-group cross sections for adjoint calculations, we utilize the BUGLE 96 multi-group [47 neutron and 20 gamma] library [19]. Further, for tallying, we use this library's group structure. For neutron source, we consider a uniform source distribution with a typical BWR spectrum.

6. Performance of A³MCNP

In our previous studies [12,13, 16], we have demonstrated that the CADIS methodology is very effective for reaction rates at a PWR cavity dosimetry. These studies, however, did not address the amount of time needed for preparing input and performing deterministic adjoint calculations.

In this paper, we will examine the performance of the code for different mesh distributions that are used for the deterministic Sn calculations. We have tested numerous Cases, and for brevity, we will discuss seven Cases with uniform meshes, and three Cases that are generated with the back-thinning utility of A³MCNP. Tables 1 and 2 represent these ten Cases.

Table 1 - Different uniform mesh Cases

Case	Total # of meshes (# axial meshes)	Mesh size (x, y, z) (cm)
1	86400 (24)	5,5,15.875
2	43200 (12)	5, 5, 31.75
3	38400 (24)	7.5,7.5,15.875
4	10800 (12)	10, 10, 31.75
5	2700 (12)	20, 20, 31.75
6	1200 (12)	30, 30, 31.75
7	300 (12)	60, 60, 31.75

Table 2 - Different back-thinned Cases

Case	No. of Meshes (axial mesh)		Max. mesh size in Fuel, moderator, steel
	Ref.	Back-thinned	
8	86400(24)	65067(24)	5.0, 10.0, 5.0
9	43200(12)	32557(12)	5.0,10.0,5.0
10	38400(24)	18525(24)	15.0,15.0,7.5

Mesh sizes of Cases 1-7 varies from 5cm to 60 m, Cases 1 and 2 have the same x-y mesh distribution and differ only in the number of z-levels, and Cases 8-10 (back thinned forms of Cases 1-3) have between 20% and 60% fewer meshes. Figs. 3a-3d show the x-y mesh distributions for Cases 1(2), 3, 8(9), and 10. Note that in the back-thinned Cases, number of x meshes varies among y-levels; this is caused by mesh recombination while considering material boundaries. Figs. 4a-4b show Cases 4-7 that have large mesh intervals, between 10 and 60 cm.

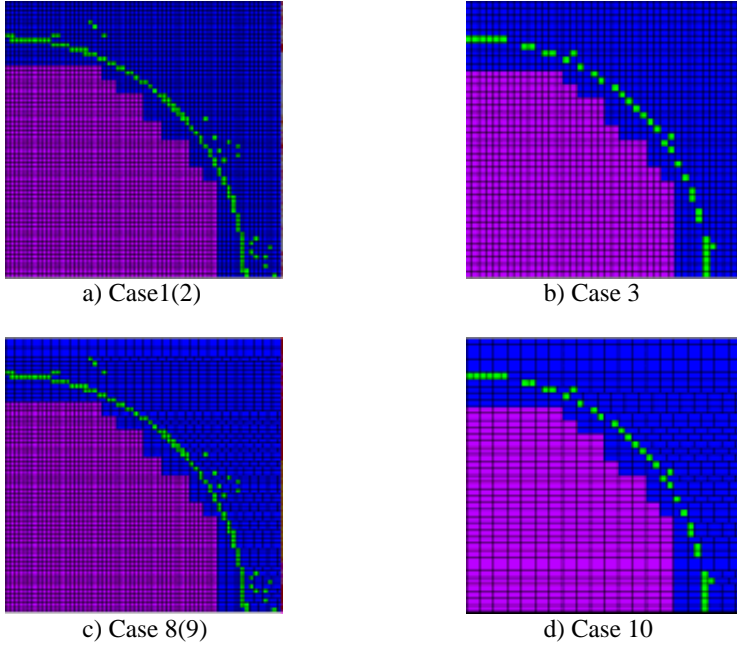


Fig. 3 - Mesh distribution for cases 1-3 and 8-10

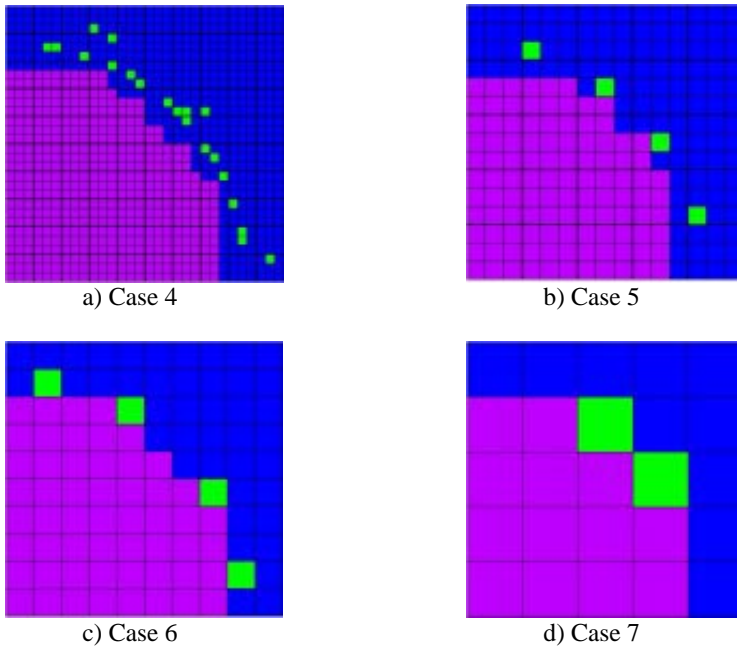


Fig. 4 - Mesh distribution for Cases 4-7

Note that in some of these Cases, because of large mesh sizes, material regions are either approximated in size/position, or omitted altogether.

Using above mesh distributions in TORT, we have performed 47-group adjoint transport calculations. Fig. 5 shows the radial adjoint function distributions at $\theta=45^\circ$ and $z=254$ cm for Case 1 for a few energy groups up to group 24 ($E>.3$ MeV). Note that beyond this group, neutron contribution to the DPA is negligible because the DPA cross sections are very small.

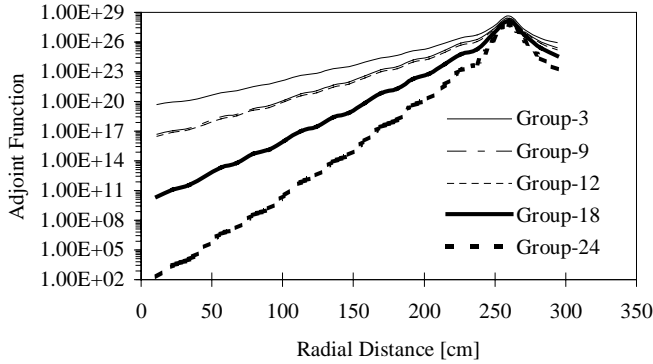


Fig. 5 - Radial adjoint function distributions of Case 1 for few groups

Fig. 6 compares the group-nine adjoint function distributions for Cases 1-3 (fine/uniform mesh) and 8-10 (back-thinned mesh). Group 9 is chosen as the representative of the groups with a large contribution to the DPA. The adjoint function distributions are similar, except for Case 10 that differs by as much as a factor of 3.

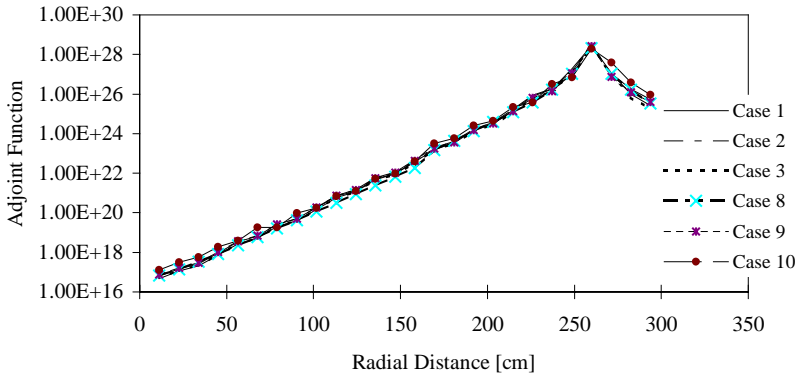


Fig. 6 - Radial adjoint function distributions for Cases 1-3 and 8-10, group 9 (3.01-3.68 MeV)

Fig. 7 compares the group-nine adjoint function distributions for Cases 1 and 4-7 (coarse meshing). As expected, due to the coarse meshing, the differences are very large (more than a few orders of magnitude). However, as it will be shown later, these very approximate distributions still yield significant speedups.

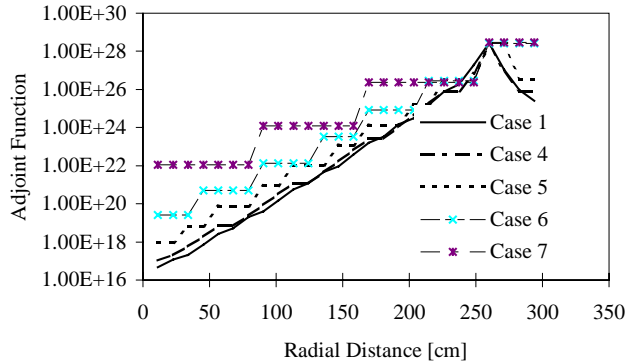


Fig. 7 - Radial adjoint function distributions for Case 1 and Cases 4-7, group 9 (3.01-3.68 MeV)

Table 3 compares the DPA values, FOM's, relative errors, and speedups of Cases 1-3 (uniform mesh) and 8-10 (back-thinned mesh) after 100 CPU minutes to the unbiased Case after 2000 CPU minutes.

Table 3 - Estimated DPA and associated statistics after 100 CPU minutes for the unbiased Case and Cases 1-3 and 8-10

Case No.	# of meshes (# of axial meshes)	DPA [dpa/sec]	Relative Error [%]	FOM	MCNP Speedup $FOM_{\text{biased}}/FOM_{\text{unbiased}}$
Unbiased	N/A	$3.877\text{E-}10^*$	14.97^*	0.022^*	1
1	86400 (24)	$3.571\text{E-}10$	1.05	90.7	4123
2	65067 (24)	$3.504\text{E-}10$	1.19	70.6	3209
3	43200 (12)	$3.452\text{E-}10$	1.26	63.1	2868
8	38400 (24)	$3.517\text{E-}10$	1.25	64.0	2909
9	32557 (12)	$3.469\text{E-}10$	1.57	40.6	1845
10	18525 (24)	$3.593\text{E-}10$	1.52	43.3	1968

* result after 2000 CPU minutes

As expected the cases with finer deterministic mesh achieve better FOMs because their adjoint function distributions are more accurate. These results, however, do not include the effect of the S_N TORT calculations. Hence, we have estimated the amount of CPU time necessary for achieving a relative error of 1% in each case, and then combined it with the corresponding S_N CPU time. Table 4 compares the total CPU times of Cases 1-3 and 8-10 to the unbiased Case.

Table 4 - Comparison of total CPU time (TORT+A₃MCNP) to achieve 1.0% (1σ) statistical uncertainty for the unbiased Case and Cases 1-3 and 8-10

Case No.	No. of meshes (# of axial meshes)	TORT [minutes]	A ³ MCNP [minutes]	Total [minutes]	Overall Speedup
Unbiased	N/A	N/A	448,201	448,201	1
1	86400 (24)	424.6	110.3	534.9	838
2	65067 (24)	309.0	141.6	450.6	995
3	43200 (12)	257.2	158.8	416.0	1077
8	38400 (24)	256.7	156.3	413.0	1085
9	32557 (12)	205.5	246.5	452.0	992
10	18525 (24)	128.7	231.0	359.7	1246

All the biased Cases result in significant speedups over the unbiased Case. Case 1 (with the most detailed mesh distribution) yields the shortest time for A³MCNP (because it uses a more accurate adjoint), but the longest total time (due to the time required for performing a more detailed TORT calculation). These results indicate that an approximate adjoint may yield a large speedup. For example, the most approximate adjoint solution among Cases 1-3 and 8-10 (i.e., Case 10) has resulted in the largest overall speedup, due to a relatively short CPU time for the Sn adjoint calculation.

Table 5 compares the DPA values, FOM's, relative errors, and speedups of Cases 4-7 (after 100 CPU minutes) to the unbiased Case (after 2000 CPU minutes).

Table 5 - Estimated DPA and associated statistics after 100 CPU minutes for the unbiased Case, and Cases 4-7

Case No.	# of meshes (# of axial meshes)	DPA [dpa/sec]	Relative Error [%]	FOM	MCNP Speedup FOM _{biased} /FOM _{unbiased}
Unbiased	N/A	3.877E-10*	14.97*	0.022*	1
4	10800 (12)	3.440E-10	1.35	54.9	2945
5	2700 (12)	3.513E-10	2.46	16.5	750
6	1200 (12)	3.512E-10	2.56	15.3	696
7	300 (12)	3.470E-10	5.88	2.89	131

* result after 2000 CPU minutes

Using the above FOM's, we have estimated the CPU time necessary for achieving a relative error of 1%. Table 6 compares the total CPU time (including deterministic (TORT Sn) and Monte Carlo (A³MCNP) calculations) for Cases 4-7 to the unbiased Case. Again, all the biased Cases result in significant speedups, even Case 7 that has a 60 cm mesh size (with a very inaccurate adjoint function) results in a noticeable speedup.

Table 6 - Comparison of total CPU time (TORT+A³MCNP) to achieve 1.0% (1σ) statistical uncertainty for the unbiased Case and Cases 4-7

Case No.	No. of meshes (# of axial meshes)	TORT [minutes]	A ³ MCNP [minutes]	Total [minutes]	Overall Speedup
Unbiased	N/A	N/A	448,201	448,201	1
4	10800(12)	40.8	182.7	223.5	2005
5	2700 (12)	10.2	604.8	615.0	729
6	1200 (12)	5.0	655.2	660.2	679
7	300 (12)	1.3	3461.4	3462.7	129

7. Summary and conclusions

We reviewed the CADIS methodology developed for automatic variance reduction of the Monte Carlo calculations. CADIS uses deterministic adjoint ("importance") function to perform source and transport biasing using the weight-window splitting/roulette methodology. We also reviewed the capabilities of A³MCNP, a new version of MCNP, which automatically prepares the necessary inputs (mesh and cross-section) for performing adjoint transport calculations. We have utilized A³MCNP to simulate a BWR core shroud. Through this problem, we have examined the performance of A³MCNP for different spatial meshing used for the deterministic adjoint calculations. Our analysis has demonstrated that for a reasonable mesh distribution, A³MCNP yields significant speedups (order of 1000) as compared to the unbiased Monte Carlo simulations. In other

words, an approximate adjoint function distribution is adequate for achieving significant variance reduction. It is also worth noting that A³MCNP significantly reduces analyst's time, while improving one's confidence in results.

References:

- [1] E.E. Lewis and W.F. Miller, Jr., *Computational Methods of Neutron Transport*, John Wiley & Sons, New York (1984).
- [2] R.R. Coveyou, V.R. Cain, and K.J. Yost, "Adjoint and Importance in Monte Carlo Applications," *Nucl. Sci. Eng.*, **27**, 219 (1967).
- [3] M.H. Kalos, "Importance Sampling in Monte Carlo Shielding Calculations: I. Neutron Penetration Through Thick Hydrogen Slabs," *Nucl. Sci. Eng.*, **16**, 227 (1963).
- [4] J.S. Tang, P.N. Stevens, and T.J. Hoffman, "Methods of Monte Carlo Biasing Using Two-Dimensional Discrete Ordinates Adjoint Flux," ORNL/TM-5414, Oak Ridge National Laboratory (1976).
- [5] M.B. Emmett, "The MORSE Monte Carlo Radiation Transport Code System," ORNL-4972, Oak Ridge National Laboratory (1975).
- [6] P.C. Miller, G.A. Wright, G.B. Boyle, and S.W. Power, "The Use of an Inbuilt Importance Generator for Acceleration of the Monte Carlo Code MCBEND," *Proc. Int. Conf. Physics of Reactor Operation, Design and Computation*, Marseilles, France, April 23-26, 1990, p.124 (1990).
- [7] S. Chucas, I. Curl, T. Shuttleworth, and G. Morrell, "Preparing the Monte Carlo Code MCBEND for the 21st Century," *Proc. 8th Int. Conf. Radiation Shielding*, Arlington, Texas, April 24-28, 1994, Vol. 1, p. 381, American Nuclear Society (1994).
- [8] M.W. Mickael, "A Fast, Automated, Semideterministic Weight Windows Generator for MCNP," *Nucl. Sci. Eng.*, **119**, 34 (1995).
- [9] J.F. Briesmeister (Ed.), "MCNP - A General Monte Carlo N-Particle Transport Code, Version 4A," LA-12625, Los Alamos National Laboratory, Los Alamos, N.M. (1993).
- [10] S.A. Turner and E.W. Larsen, "Automatic Variance Reduction for 3-D Monte Carlo Simulations by the Local Importance Function Transform," *Trans. Am. Nucl. Soc.*, **75**, 131 (1996).
- [11] K.A. Van Riper et al., "AVATAR - Automatic Variance Reduction in Monte Carlo Calculations," *Proc. Joint. Int. Conf. Mathematical Methods and Supercomputing for Nuclear Applications*, Saratoga Springs, New York, October 6-10, 1997, Vol. 1, p. 661, American Nuclear Society (1997).
- [12] J.C. Wagner, "Acceleration of Monte Carlo Shielding Calculations with an Automated Variance Reduction Technique and Parallel Processing," *Ph.D. Thesis*, The Pennsylvania State University (1997).
- [13] J.C. Wagner and A. Haghghat, "Automated Variance Reduction of Monte Carlo Using the Discrete Ordinates Adjoint Function," *Nucl. Sci. Eng.*, **128**, 186 (1998).
- [14] J.C. Wagner and A. Haghghat, "A³MCNP, Automated Adjoint Accelerated MCNP - User's Manual," The Pennsylvania State University (April 1997, revised Aug. 1998).

- [15] W.A. Rhoades and D.B. Simpson, "The TORT Three-Dimensional Discrete Ordinates Neutron/Photon Transport Code," ORNL/TM-11778, Oak Ridge National Laboratory (1997).
- [16] B.G. Petrovic, J. C. Wagner, and A. Haghghat, "Verification of Improved Synthesized 3-D S_N and Monte Carlo Methods for Pressure Vessel Fast Neutron Fluence Calculations," *Proc. Joint Int. Conf. on Mathematical Methods and Supercomputing for Nuclear Applications*, Saratoga Springs, New York, October 6-10, 1997, Vol. 2, p. 1586, American Nuclear Society (1997).
- [17] M.H. Kalos and P. A. Whitlock, *Monte Carlo Methods, Vol. I: Basics*, John Wiley and Sons (1986).
- [18] W.A. Rhoades and M.B. Emmett, "DOS: The Discrete Ordinates System," ORNL/TM-8362, Oak Ridge National Laboratory (1982).
- [19] J.E. White et al., "BUGLE-96: A Revised Multigroup Cross Section Library for LWR Applications Based on ENDF/B-VI Release 3," *Proc. Tpl. Mtg. Radiation Protection and Shielding*, No. Falmouth, Massachusetts, April 21-25, 1996, Vol. 2, p. 1071, American Nuclear Society (1996).